

Aging and other related phenomena in potassium niobo-tantalate crystals studied through the frequency dependence of their dielectric constant

This article has been downloaded from IOPscience. Please scroll down to see the full text article.

2001 J. Phys.: Condens. Matter 13 8799

(<http://iopscience.iop.org/0953-8984/13/39/308>)

View [the table of contents for this issue](#), or go to the [journal homepage](#) for more

Download details:

IP Address: 171.66.16.226

The article was downloaded on 16/05/2010 at 14:55

Please note that [terms and conditions apply](#).

Aging and other related phenomena in potassium niobo-tantalate crystals studied through the frequency dependence of their dielectric constant

P Doussineau¹, T de Lacerda-Arôso² and A Levelut¹

¹ Laboratoire des Milieux Désordonnés et Hétérogènes³, Université P et M Curie, Case 86, 75252 Paris Cédex 05, France

² Departamento de Física, Universidade do Minho, 4709 Braga, Portugal

Received 26 April 2001, in final form 27 July 2001

Published 13 September 2001

Online at stacks.iop.org/JPhysCM/13/8799

Abstract

We report on dielectric measurements in the frequency range from 1 to 1000 kHz in two disordered ferroelectric $\text{KTa}_{1-y}\text{Nb}_y\text{O}_3$ (KTN) crystals ($y \cong 0.02$). We have studied the frequency dependence of the dielectric constant (real and imaginary parts) during several thermal evolutions: isothermal aging, rejuvenation by cooling or heating after a temperature plateau, memory. In every case the frequency dependence is well described by a power law. The temperature and plateau duration dependences of the exponents have been studied. We give a description of our results within a model where the variations of the dielectric constant are attributed to the motion (growth and reformation) of ferroelectric domain walls. In particular we are able to explain the identity of the exponents of the frequency power law dependence of memory and isothermal aging.

1. Introduction

Disordered materials are in general out of equilibrium systems. As a consequence, at fixed temperature they relax slowly towards a more ordered state; this is aging. Aging has been observed in polymers [1], spin glasses [2–4], supercooled liquids [5], disordered dielectrics [6–10], relaxor ferroelectrics [11] and colloidal glasses [12, 13]. Some other phenomena are commonly associated with aging. If, after aging at a given temperature T_{pl} which induces a decrease of some susceptibility, the system is cooled or heated, evolution towards a more disordered state is often observed; this is rejuvenation. Finally after cooling and subsequent heating the susceptibility presents a dip at T_{pl} ; this is memory. Rejuvenation and memory have been observed in spin glasses [14, 15], disordered ferroelectrics [16] and disordered

³ Associated with the Centre National de la Recherche Scientifique (UMR 7603).

ferromagnets [17], polymers [18, 19] and relaxor ferroelectrics [11] but not in a disordered paraelectric [20]. Up to now, there is no model able to describe all these results.

In this paper we focus our attention on the behaviour of potassium niobo-tantalate $\text{KTa}_{1-y}\text{Nb}_y\text{O}_3$ (KTN) crystals. At low temperatures, KTN crystals are in a disordered (because of the randomly substituted niobium atoms) ferroelectric phase and they show effective ergodicity breaking, rejuvenation and memory [10, 16]. In another neighbouring family of disordered dielectrics, the potassium–lithium tantalate $\text{K}_{1-x}\text{Li}_x\text{TaO}_3$ (KLT) crystals, which are in a paraelectric phase at low temperatures, effective ergodicity breaking was observed but neither rejuvenation nor memory [7, 20]. It is worth noticing that all the features observed in KLT are nearly independent of frequency [7], specially at low temperatures while they appear frequency dependent in KTN [10].

In order to explain the KLT behaviour a model was proposed [8, 9]. In this model, the time-dependent part $\delta\varepsilon(\omega, t)$ of the dielectric constant at frequency $f = \omega/(2\pi)$ is attributed to the slow growth, hindered by static random fields, of polarization domains in the tantalate lattice. The domain size $R(T, t)$ is limited by the temperature-dependent coherence length $\xi(T)$ of the fluctuations, which stays finite in the whole experimental temperature range. The model is very simple since it assumes that the aging properties of every domain are characterized by the unique parameter $R(T, t)$. However, in order to describe some non-monotonic behaviour, it is necessary to introduce a size distribution.

In this paper we report on a detailed study of aging, rejuvenation, memory and some other effects studied by the means of the frequency dependence of the dielectric constant of KTN and we propose a modified domain model able to account for most of the observed features: we assume that every domain is not fully characterized by its main size $R(T, t)$ alone, but that its shape (or conformation) also plays a role.

If aging is observed in many materials, the analogy is strongest between the features observed in the KTN family and those in spin glasses, in particular the trio aging–rejuvenation–memory. Moreover, it is generally assumed that in both cases the origin of the effects are disorder and frustration in the interactions between electric dipoles or spins. Therefore, a comparison of these two families should be most interesting, with one advantage in favour of KTN: the ferroelectric phase is probably better known than the spin-glass phase.

Before proceeding to a detailed analysis of our data, we emphasize that the major feature observed when the temperature is decreased from the transition temperature T_{tr} to low temperatures is a large immediate decrease of the dielectric constant. This is not our main interest. Indeed, we focus our attention on much smaller variations, which depend on time and on the thermal history of the sample. This is the real object of this paper.

A short preliminary report has been published [21]. The already published results are quoted but not reproduced here. Moreover, since many quantities show similar behaviours, all the observed features are mentioned but only some of them, chosen as illustrative examples, are reported in detail and sketched in figures.

2. Experiments

The pure potassium tantalate KTaO_3 crystal is a cubic perovskite. It is an incipient ferroelectric: the ferroelectric transition it would undergo at 0 K is aborted, due to quantum fluctuations. However, the dielectric constant ε strongly rises as the temperature is lowered since the correlations between the displacements of the tantalum ions increase. The random substitution of Nb^{5+} ions to Ta^{5+} ions in a KTaO_3 crystal has two consequences. Firstly, the Nb^{5+} ions take off-centre positions and constitute electric dipoles located on random sites and oriented at random along one of the eight [111] directions. Secondly, the trend of the tantalate

lattice towards ferroelectricity is enhanced: the ferroelectric transition is shifted from 0 K for pure KTaO_3 to the finite temperature T_{tr} , close to 30 K if the niobium concentration is around 2% [22]. In the temperature range of our experiments the ferroelectric phase has the rhombohedral symmetry but its growth towards a unique domain over all the sample is prevented by the static random fields generated by the Nb^{5+} ions. Therefore, the domain sizes are small in comparison with the sample size. Moreover, the eight possible types of rhombohedral domain are equally probable in absence of biasing electric field. Consequently, the sample is macroscopically cubic and its dielectric constant is isotropic.

Using a Hewlett–Packard 4192A impedance analyser, we have measured the electric capacitance and the loss when the frequency f lies in the range between 1 kHz and 1 MHz. They can be changed into the complex capacitance $C = C' - iC''$, which, in turn, can be transformed into the complex dielectric constant $\varepsilon = \varepsilon' - i\varepsilon''$. The real part ε' and the imaginary part ε'' are simply proportional to the real capacitance C' and to the imaginary capacitance C'' , respectively. In the present experiments the complex dielectric constant $\varepsilon(T, t, f) = \varepsilon'(T, t, f) - i\varepsilon''(T, t, f)$ has been measured as a function of the frequency f and the time t while the sample temperature $T(t)$ was a controlled function of time.

The amplitude of the oscillating electric field was $E \cong 1.2 \text{ kV m}^{-1}$ at any frequency. In such a field, non-linearities are observable in the vicinity of the transition but they are negligible in the temperature range (below 15 K) of the present experiments [10].

In this paper we analyse the data obtained at different frequencies, for several plateau temperatures and various plateau durations on two KTN samples, one with the niobium concentration $y = 0.022$ and transition temperature $T_{tr} = 31 \text{ K}$ (sample A), the second with $y = 0.027$ and $T_{tr} = 38 \text{ K}$ (sample B). These two samples have been already used in previous works [10, 16, 25]. The proportionality factors between their capacitances and their dielectric constants are such that $C = 1 \text{ pF}$ corresponds to $\varepsilon \cong 20$ for sample A and $\varepsilon \cong 16$ for sample B. Dielectric constant values measured at $f = 1 \text{ kHz}$ on sample B are as follows: $\varepsilon' \cong 42\,000$ and $\varepsilon'' \cong 7\,000$ at T_{tr} , $\varepsilon' \cong 2\,900$ and $\varepsilon'' \cong 70$ when arriving at $T_{pl} = 11.2 \text{ K}$ while the aging decreases at this temperature during $t_{pl} = 2\,000 \text{ s}$ are $\Delta\varepsilon' \cong 60$ and $\Delta\varepsilon'' \cong 12$.

All our experiments begin with annealing the sample near 55 K and rapidly cooling it across the transition temperature T_{tr} down to $T_{ch} \cong 22 \text{ K}$ where the cooling rate is changed. Then several procedures were used. They were composed of a cooling at a constant rate $dT/dt = -r = r_c$, a heating at the opposite rate $dT/dt = +r = r_h$ and a temperature plateau T_{pl} maintained during t_{pl} . These three components were combined in different manners explained in detail in section 5.1. For our experiments we had $r = 5.2 \text{ mK s}^{-1}$. Three temperatures play particular roles: T_{min} , $T_{ch} \cong 22 \text{ K}$ and T_{pl} between them. In contrast to the case of KLT, the curves recorded in KTN at different measuring frequencies are different. Consequently, the measuring frequency is a relevant parameter; it is the main object of the present study.

3. Preliminary remark

Before we present our data, we indicate the main lines of our results and analysis. For a given plateau temperature and a given plateau duration, we measure various aging (i.e. time dependent) complex quantities $X(T, t, f)$ which all obey negative power laws with respect to the frequency f , at least in all our measurement range. Such a behaviour is related to the so-called Curie–von Schweidler response function

$$\tilde{\chi}(t) = \frac{Y(t)}{\Gamma(\sigma)\tau} \left(\frac{t}{\tau}\right)^{\sigma-1}$$

indeed first introduced by F Kohlrausch as early as 1863. The Fourier transform of $\tilde{\chi}(t)$ is the susceptibility

$$\chi(\omega) = [\cos(\pi\sigma/2) - i \sin(\pi\sigma/2)](\omega\tau)^{-\sigma}$$

where $\omega = 2\pi f$ is the circular frequency and τ is some relaxation time. This form can be obtained in the framework of the linear, stationary and causal response theory, and therefore it satisfies the Kramers–Krönig relations. We write the real part $X'(T, t, f)$ and the imaginary part $X''(T, t, f)$ of $X(T, t, f)$ as

$$X'(T, t, f) = S'(T, t) f^{-\sigma(T,t)} \text{ and } X''(T, t, f) = S''(T, t) f^{-\sigma(T,t)}$$

where the two amplitudes S' and S'' and the exponent σ depend on T and t but not on f . Two properties have to be underlined: (i) the two parts X' and X'' have the same frequency dependence; (ii) the ratio $X''/X' = S''/S' = \tan(\pi\sigma/2)$ depends only on the exponent σ .

It could be thought that there is some contradiction in using a susceptibility which satisfies the Kramers–Krönig relations while depending both on frequency and on time and therefore exhibiting non-stationarity. Indeed, such a form is a valid approximation since there are two very different time scales: from one microsecond to one millisecond for the oscillating field and typically one kilosecond for the slow evolution (aging).

Since our measurements on the real part are more accurate than those on the imaginary part, we make use of the two previous properties as follows. We accurately determine σ from the behaviour of the real part. Then we calculate $\tan(\pi\sigma/2)$ and we plot on a log–log scale the real part X' and the imaginary part X'' divided by $\tan(\pi\sigma/2)$ as a function of f . The two sets of data points must be superimposed. If they are, this is a check of the coherence of the analysis and of the appropriateness of the function.

4. Frequency analysis of isothermal aging

The isothermal time variation of the complex dielectric constant $\varepsilon(T, t, f)$ in KTN is a slow decay of both its parts which depends on the cooling rate r_c . In particular, the asymptotic value of ε , extrapolated by a fit on very long time measurements, exhibits effective ergodicity breaking [10]. In our experiments, aging depends on three parameters: the plateau duration t_{pl} , the plateau temperature $T_{pl} < T_r$ and the measuring frequency f . We have examined the role of each of them.

For a given plateau temperature and a given plateau duration, the variation $\Delta\varepsilon(T_{pl}, t_{pl}, f) = \varepsilon(T_{pl}, t_{pl}, f) - \varepsilon(T_{pl}, 0, f)$ of the complex dielectric constant obeys a negative power law of the frequency f . We respectively write the real part and the imaginary part of the variation as

$$\Delta\varepsilon'(T_{pl}, t_{pl}, f) = -N' f^{-\nu} \text{ and } \Delta\varepsilon''(T_{pl}, t_{pl}, f) = -N'' f^{-\nu}$$

where the amplitudes N' and N'' and the exponent ν depend on T_{pl} and t_{pl} but not on f . Then we apply the analysis procedure explained above. These results obtained on sample A have been already published [21].

The exponent ν is of the order of 0.2 and it depends on both temperature and time. More precisely, for $T_{pl} = 12.1$ K it varies as $\nu \cong 0.28 - 0.033 \log t_{pl}$, with t_{pl} in seconds; the equation leads to $\nu = 0$ when $t_{pl} \cong 10$ years, much beyond the domain where it was established. For $t_{pl} = 10\,000$ s it varies as $\nu \cong 0.22 - 0.063 T_{pl}$, with T_{pl} in kelvin. We notice that for the shortest durations for which the word plateau still has a meaning ($t_{pl} \approx 50$ – 100 s), the exponent becomes nearly independent of T_{pl} and its value is $\nu = 0.23 \pm 0.005$.

The magnitudes N' and N'' are increasing functions of T_{pl} and t_{pl} . Their increase with t_{pl} is isothermal aging; it becomes slower and slower as long as time elapses.

5. Frequency analysis of thermal evolution

5.1. Analysis method

The analysis method used here was initially developed for KLT crystals for the response to temperature and time changes [20]. In those materials the measuring frequency f only plays a weak role, which has not been examined. In contrast, in KTN crystals the effects strongly depend on f . We first recall the analysis method, applied here for every frequency.

We have studied the variations of the complex dielectric constant $\varepsilon(T, t, f)$ in the vicinity of several remarkable points (T_0, t_0) in the (T, t) plane. Except during the plateau, the temperature changes are proportional to the time changes: between them the relationship is either $T - T_0 = r_c(t - t_0)$ for cooling or $T - T_0 = r_h(t - t_0)$ for heating. Therefore, in the expansion

$$\varepsilon(T, t, f) = \varepsilon(T_0, t_0, f) + \left(\frac{\partial \varepsilon}{\partial T}\right)_t (T - T_0) + \left(\frac{\partial \varepsilon}{\partial t}\right)_T (t - t_0) + \dots$$

we put

$$\left(\frac{\partial \varepsilon}{\partial T}\right)_z = \left(\frac{\partial \varepsilon}{\partial T}\right)_t + \frac{1}{r_z} \left(\frac{\partial \varepsilon}{\partial T}\right)_T$$

and we obtain

$$\varepsilon(T, t, f) = \varepsilon(T_0, t_0, f) + \left(\frac{\partial \varepsilon}{\partial T}\right)_z (T - T_0) + O((T - T_0)^2)$$

where z stands for c or h . All the derivatives are taken at (T_0, t_0) . For more clarity we write

$$\varepsilon(T, t, f) = \varepsilon(T_0, t_0, f) + \hat{P}(T_0, t_0, f)_z (T - T_0) + O((T - T_0)^2).$$

For the isothermal plateau we conventionally put

$$\left(\frac{\partial \varepsilon}{\partial T}\right)_z = 0 + \frac{1}{|r_z|} \left(\frac{\partial \varepsilon}{\partial T}\right)_T$$

and consequently, the previous equation is also valid in this case. Therefore, we can treat the case of the plateau, although isothermal, in the present section.

We take as time origin the instant when the plateau temperature T_{pl} is reached. Therefore, the beginning of the plateau corresponds to $t_0 = 0$ and the end to $t_0 = t_{pl}$.

The variation $d\varepsilon = \varepsilon(T, t, f) - \varepsilon(T_0, t_0, f)$ is determined along some paths in the (T, t) plane. The different paths are referred to according to the following notation. The points $(T_{pl}, 0)$ and (T_{pl}, t_{pl}) are respectively called points 1 and 2. The letters c and h mean cooling and heating while the letters a and b mean above and below, respectively. An isothermal path is labelled by pl . Hence, for instance, path $ca-1$ leads to point 1 by cooling from above while path $pl-2$ arrives at point 2 along the plateau. The possible paths in the vicinity of points 1 and 2 are drawn in figure 1.

The four different procedures used were the following sequences:

- (i) cooling from T_{ch} to T_{pl} (path $ca-1$) + heating from T_{pl} to T_{ch} (path $ha-1$);
- (ii) cooling from T_{ch} to T_{pl} (path $ca-1$) + plateau at T_{pl} + heating from T_{pl} to T_{ch} (path $ha-2$);
- (iii) cooling from T_{ch} to T_{min} (path $ca-1$ + path $cb-1$) + heating from T_{min} to T_{ch} ;
- (iv) cooling from T_{ch} to T_{pl} (path $ca-1$) + plateau at T_{pl} + cooling from T_{pl} to T_{min} (path $cb-2$) + heating from T_{min} to T_{ch} .

As already mentioned, any temperature change is followed by a large immediate dielectric constant change, which is not our main interest in the present paper. In order to eliminate this parasitic effect we study the difference of the variation along two convenient paths.

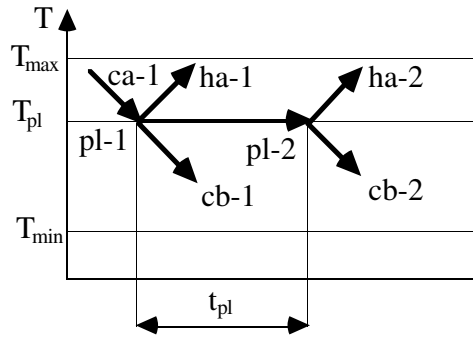


Figure 1. Schematic representation of the four thermal histories used in our experiments. The arrows indicate the direction of the temperature variation. (a) Path *ca-1* + path *ha-1*: cooling from T_{ch} down to T_{pl} and subsequent heating from T_{pl} up to T_{ch} ; path *ca-1* + plateau at T_{pl} + path *ha-2*: cooling from T_{ch} down to T_{pl} , isotherm and heating from T_{pl} up to T_{ch} . (b) Path *ca-1* + path *cb-1*: cooling from T_{ch} down to T_{min} ; path *ca-1* + plateau at T_{pl} + path *cb-2*: cooling from T_{ch} down to T_{pl} , isotherm and cooling from T_{pl} down to T_{min} .

5.2. On the plateau at T_{pl}

We first examined the isothermal ($r = 0$) variation of $\varepsilon(T, t, f)$ on the plateau. Such a path corresponds to $(T_{pl}, t) \rightarrow (T_{pl}, t + \delta t)$. The complex dielectric constant change is

$$d\varepsilon_{pl} = \varepsilon(T_{pl}, t + \delta t, f) - \varepsilon(T_{pl}, t, f) = Q(T_{pl}, t, f)\delta t < 0$$

with

$$Q(T_{pl}, t, f) = \left(\frac{\partial \varepsilon}{\partial t} \right)_T.$$

We notice that the present method is differential while the interpretation given in section 4 is integral. Indeed, they are related by

$$\Delta \varepsilon(T_{pl}, t_{pl}, f) = \int_0^{t_{pl}} dt Q(T_{pl}, t, f).$$

Consequently, from what we know of $\Delta \varepsilon(T_{pl}, t_{pl}, f)$ (see section 4), we may guess that $Q(T_{pl}, t, f)$ depends on f . The real part at the beginning of the plateau is found to follow the power law

$$Q'(T_{pl}, 0, f) = -L'(T_{pl}, 0) f^{-\lambda(T_{pl}, 0)}.$$

In fact, it is determined by a mean value over $t_{pl} \cong 0-60$ s. For $T_{pl} = 12.1$ K, we get $\lambda = 0.23 \pm 0.01$ (figure 2). Indeed, in the temperature range where our accuracy is good enough ($10 \text{ K} \leq T_{pl} \leq 14 \text{ K}$) it was found that $\lambda = 0.23 \pm 0.02$ whatever T_{pl} is. In order to roughly estimate the variation with t_{pl} , we have calculated that $\lambda \cong 0.15$ for $t_{pl} = 1000$ s. For the imaginary part $Q''(T_{pl}, 0, f)$ and for the real part if $t_{pl} > 5000$ s, the evolution is very slow and we cannot get reliable measurements.

5.3. Below the plateau

Now we examine the paths *cb-1* and *cb-2*, which are below T_{pl} . The plateau is the only difference between their thermal histories. The expansion of the complex dielectric constant

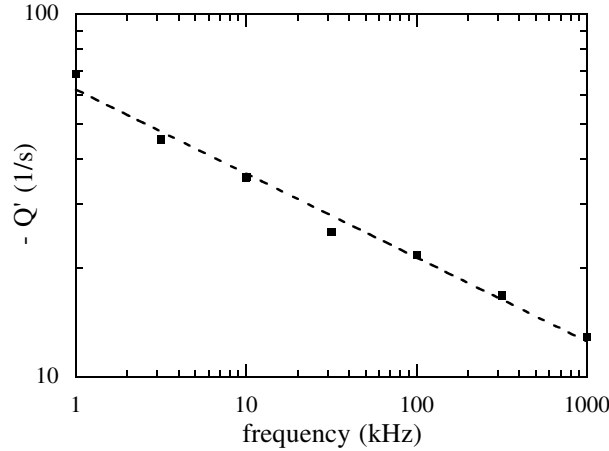


Figure 2. Derivative $Q' = dC'/dt$ (calculated for $t_{pl} \rightarrow 0$, with its sign changed) as a function of frequency on a log–log plot measured in sample A at T_{pl} 12.1 K. The slope of the fitting line is the exponent $\lambda \cong 0.23$.

difference at the temperature $T < T_{pl}$ reads

$$d(\varepsilon_{cb-2} - \varepsilon_{cb-1}) = [\varepsilon(T_{pl}, t_{pl}, f) - \varepsilon(T_{pl}, 0, f)] \\ + [\hat{P}(T_{pl}, t_{pl}, f)_c - \hat{P}(T_{pl}, 0, f)_c](T - T_{pl}) + O((T - T_{pl})^2).$$

We have found that the coefficient of the second term has the following form:

$$\hat{P}(T_{pl}, t_{pl}, f)_c - \hat{P}(T_{pl}, 0, f)_c = D\hat{P}(T_{pl}, t_{pl}, f)_c = -B(T_{pl}, t_{pl})f^{-\beta(T_{pl}, t_{pl})}.$$

Clearly, from this definition $B(T_{pl}, 0) = 0$. The complex magnitude B and the exponent β depend on T_{pl} and t_{pl} . In this case, the accuracy on the loss is good and we are able to actually measure the two parts of the complex dielectric constant. In figure 3 the real part $-D\hat{P}'(T_{pl}, t_{pl}, f)_c$ is displayed with the fitting straight line, the slope of which is the exponent β . For $T_{pl} = 14.3$ K and $t_{pl} = 10\,000$ s this leads to $\beta \cong 0.20$ and $\tan(\pi\beta/2) \cong 0.33$. In the same figure the imaginary part $-D\hat{P}''(T_{pl}, t_{pl}, f)_c$ and the ratio $-D\hat{P}''(T_{pl}, t_{pl}, f)_c / \tan(\pi\beta(T_{pl}, t_{pl})/2)$ of the imaginary part divided by the number $\tan(\pi\beta/2)$ are shown as a function of the frequency f where the exponent β is obtained by direct calculation from $D\hat{P}'(T_{pl}, t_{pl}, f)_c$. A quite good superposition of the first and the third data sets is obtained.

We have found that the exponent β does not depend on the time t_{pl} but it weakly increases with the plateau temperature, according to $\beta \cong 0.07 + 0.009T_{pl}$, with T_{pl} in kelvin, at least between 7 K and 15 K. The magnitudes $B'(T_{pl}, t_{pl})$ and $B''(T_{pl}, t_{pl})$ are increasing functions of T_{pl} and t_{pl} . This leads to

$$B(T_{pl}, t_{pl}) = -D\hat{P}(T_{pl}, t_{pl}, f)_c f^{+(0.07+0.009T_{pl})}.$$

Obviously, $D\hat{P}(T_{pl}, t_{pl}, f)_c$ is equal to 0 if $t_{pl} = 0$. Moreover, the difference $D\hat{P}(T_{pl}, t_{pl}, f)_c$ is negative and increases with t_{pl} for long t_{pl} . This means that it passes through an extremum. For $T_{pl} = 12.1$ K the exponent is $\beta \cong 0.18$. At this temperature, for long t_{pl} we have displayed on a log–log scale the two quantities B' and $B'' / \tan(\pi\beta/2)$ for $f = 10$ kHz and the quantity B' for $f = 100$ kHz as a function of t_{pl} for $t_{pl} \geq 2000$ s. As expected, the data points of these three quantities are quite well superimposed (see figure 4), thus showing

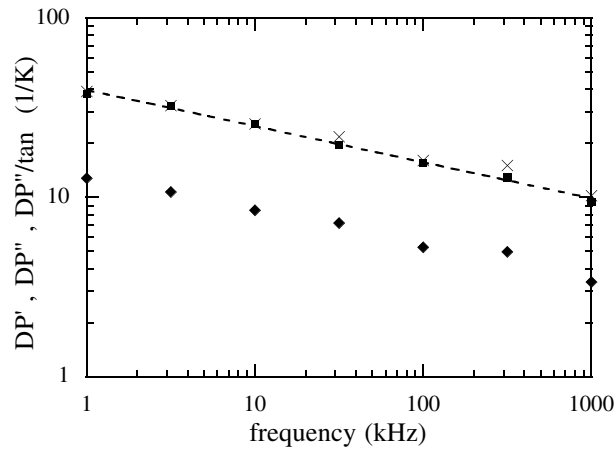


Figure 3. Log–log plot of the complex coefficient DP as a function of the frequency f measured in sample A for $T_{pl} = 14.3$ K and $t_{pl} = 10\,000$ s. Three quantities are sketched: (i) the real part DP' (squares) with its fit by a straight line, the slope of which is the exponent $\beta \cong 0.20$; (ii) the imaginary part DP'' (diamonds); (iii) the imaginary part divided by $\tan(\pi\beta/2)$ (crosses). The superposition of squares and crosses is a good test of the power law $f^{-\beta}$.

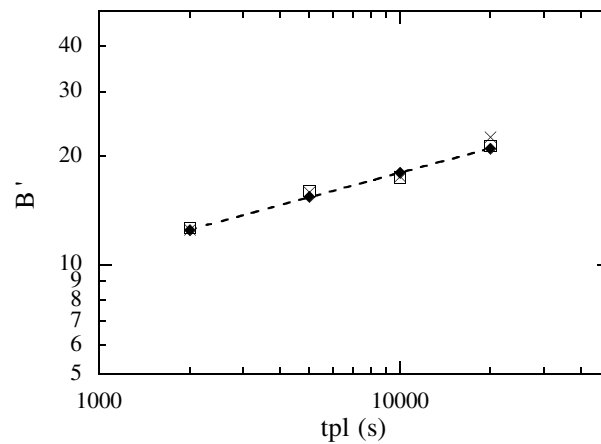


Figure 4. Log–log plot of the complex coefficient B as a function of the plateau duration t_{pl} measured in sample A at $T_{pl} = 12.1$ K. Three quantities are sketched: on the one hand, the real part B' (open squares) and the imaginary part B'' divided by $\tan(\pi\beta/2)$ (crosses) both at $f = 10$ kHz; on the other hand the real part B' (diamonds) at $f = 100$ kHz. The superposition of the data points shows that B does not depend on frequency. The fitting line provides the variation $B \propto t_{pl}^{+0.23}$.

that they are independent of f . The common slope provides a variation proportional to $t_{pl}^{+0.23}$. Finally, we have found

$$D\hat{P}(T_{pl}, t_{pl}, f)_c \propto t_{pl}^{+0.23} f^{-0.18} \text{ for } T_{pl} = 12.1 \text{ K and } t_{pl} \geq 2000 \text{ s}$$

where the two exponents depend on T_{pl} .

When they are displayed on a logarithmic scale as a function of T_{pl} on a linear scale, for $t_{pl} = 10\,000$ s the data points of the same three quantities as in figure 4 are on a straight line

(not shown). From its slope we deduce that $B(T_{pl}, t_{pl}) \propto \exp(0.33T_{pl})$. Finally, we obtain

$$D\hat{P}(T_{pl}, t_{pl}, f)_c \propto -\exp(0.33T_{pl})f^{-(0.07 \pm 0.009T_{pl})} \text{ for } t_{pl} = 10\,000 \text{ s.}$$

5.4. Above the plateau

Now we examine the paths $ha-1$ and $ha-2$, which are above T_{pl} . The only difference between the thermal histories of these two paths is the plateau. The expansion of the complex dielectric constant difference at the temperature $T > T_{pl}$ reads

$$\begin{aligned} d(\varepsilon_{ha-2} - \varepsilon_{ha-1}) &= [\varepsilon(T_{pl}, t_{pl}, f) - \varepsilon(T_{pl}, 0, f)] \\ &\quad + [\hat{P}(T_{pl}, t_{pl}, f)_h - \hat{P}(T_{pl}, 0, f)_h](T - T_{pl}) + O((T - T_{pl})^2). \end{aligned}$$

We have found that the coefficient of the second term has the following form:

$$\hat{P}(T_{pl}, t_{pl}, f)_h - \hat{P}(T_{pl}, 0, f)_h = D\hat{P}(T_{pl}, t_{pl}, f)_h = A(T_{pl}, t_{pl})f^{-\alpha(T_{pl}, t_{pl})}.$$

Clearly, from this definition $A(T_{pl}, 0) = 0$. The complex magnitude A depends on T_{pl} and t_{pl} . The exponent α is found to be independent of the plateau temperature and duration; its value is $\alpha = 0.275 \pm 0.02$.

Obviously, $D\hat{P}(T_{pl}, t_{pl}, f)_h$ is equal to 0 if $t_{pl} = 0$ whatever T_{pl} is. Moreover, the two parts of the difference $D\hat{P}(T_{pl}, t_{pl}, f)_h$ are positive and are decreasing functions of t_{pl} for long t_{pl} . This means that they pass through an extremum. This was already observed in our previous experiments [16]. For long t_{pl} we have found

$$D\hat{P}(T_{pl}, t_{pl}, f)_h \propto t_{pl}^{-0.12} \text{ for } T_{pl} = 12.1 \text{ K and } t_{pl} \geq 2000 \text{ s}$$

independently of frequency, as expected.

We now examine the variation with T_{pl} for $t_{pl} = 10\,000$ s. In figure 5 we have displayed on a logarithmic scale the quantity A' measured at $f = 10$ kHz and $f = 100$ kHz as a function of T_{pl} on a linear scale. The data points are on a straight line. From its slope we deduce that $A \propto \exp(0.36T_{pl})$. Finally, we obtain

$$D\hat{P}(T_{pl}, t_{pl}, f)_h \propto \exp(0.36T_{pl})f^{-0.275} \text{ for } t_{pl} = 10\,000 \text{ s.}$$

5.5. Immediate heating after cooling down to T_{pl}

The paths $ca-1$ and $ha-1$ which are above T_{pl} are convergent on point 1. The expansion of the complex dielectric constant change at the temperature $T > T_{pl}$ reads

$$d(\varepsilon_{ha-1} - \varepsilon_{ca-1}) = [\hat{P}(T_{pl}, 0, f)_h - \hat{P}(T_{pl}, 0, f)_c](T - T_{pl}) + O((T - T_{pl})^2).$$

We have found that the coefficient of the first term has the following form:

$$\hat{P}(T_{pl}, 0, f)_h - \hat{P}(T_{pl}, 0, f)_c = D\hat{P}(T_{pl}, 0, f)_{h-c} = -M(T_{pl})f^{-\mu(T_{pl})}.$$

The complex magnitude M and the exponent μ depend on T_{pl} . Figure 6 shows our data concerning the dominant term. For $T_{pl} = 12.1$ K they provide the value $\mu = 0.13 \pm 0.01$. The exponent μ depends on temperature; it is quite well represented by the linear law $\mu \approx 0.26 - 0.01T_{pl}$. This leads to the useful form

$$M(T_{pl}) = -D\hat{P}(T_{pl}, 0, f)_{h-c}f^{+(0.26-0.01T_{pl})}.$$

From the study of the product $D\hat{P}'_c f^\mu$, which must be independent of f , as a function of T_{pl} , we deduce that $M(T_{pl}) \propto \exp(0.3T_{pl})$. Finally, we obtain

$$D\hat{P}'(T_{pl}, 0, f)_{h-c} \propto -\exp(0.3T_{pl} - 0.26 \ln f + 0.01T_{pl} \ln f).$$

This means that even in this simple case where $t_{pl} = 0$, the function $D\hat{P}'(T_{pl}, 0, f)_{h-c}$ is not separable with respect to the two variables T_{pl} and f .

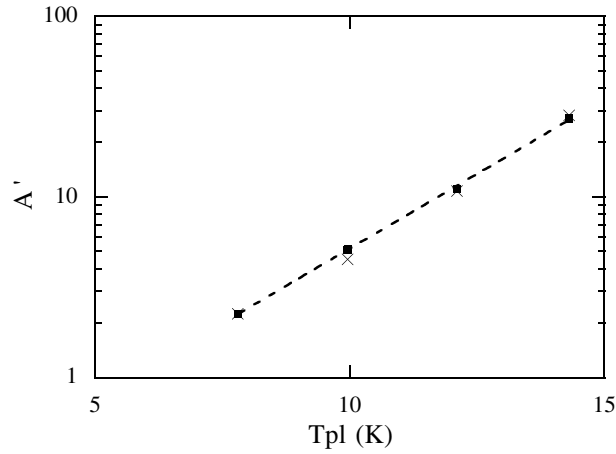


Figure 5. Semi-logarithmic plot of the real part A' of the complex coefficient A as a function of the plateau temperature T_{pl} , measured at $f = 10$ kHz (squares) and $f = 100$ kHz (crosses) in sample A for $t_{pl} = 10\,000$ s. From the fit it is deduced that $A \propto \exp(0.36T_{pl})$, independently of frequency.

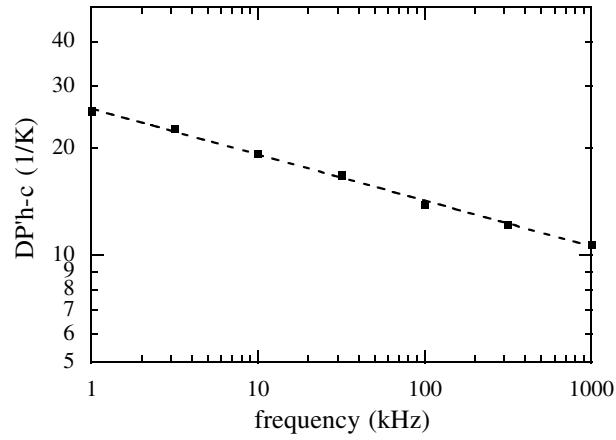


Figure 6. Log-log plot of the real part $DP'h-c$ of the complex coefficient $DP'h-c$ as a function of the frequency f measured in sample A. The fit gives the exponent $\mu \simeq 0.13$.

6. Frequency analysis of rejuvenation and derivability breaking

We turn now towards the question of rejuvenation upon cooling after aging, for which we need a precise definition. We obtain it through two conditions on the complex coefficient P (without circumflex) [23]. Starting from

$$-B(T_{pl}, t_{pl}) f^{-\beta(T_{pl}, t_{pl})} = \hat{P}(T_{pl}, t_{pl}, f)_c - \hat{P}(T_{pl}, 0, f)_c$$

we obtain

$$P(T_{pl}, t_{pl}, f)_c - P(T_{pl}, 0, f)_c = -B(T_{pl}, t_{pl}) f^{-\beta(T_{pl}, t_{pl})} - \frac{1}{r_c} [Q(T_{pl}, t_{pl}, f) - Q(T_{pl}, 0, f)].$$

Rejuvenation exists if and only if the two conditions

$$P^*(T_{pl}, t_{pl}, f)_c - P^*(T_{pl}, 0, f)_c < 0$$

where the star stands for prime or double prime, hold [23]. In terms of measured quantities, they read

$$B^*(T_{pl}, t_{pl})f^{-\beta(T_{pl}, t_{pl})} + (1/r_c)[Q^*(T_{pl}, t_{pl}, f) - Q^*(T_{pl}, 0, f)] > 0.$$

The first term is positive; the term in brackets is positive too, while its factor $(1/r_c)$ is negative.

In analogy with what was done for cooling after aging, the two conditions for rejuvenation upon heating after aging [23] read

$$P^*(T_{pl}, t_{pl}, f)_h - P^*(T_{pl}, 0, f)_h > 0.$$

With

$$P(T_{pl}, t_{pl}, f)_h - P(T_{pl}, 0, f)_h = A(T_{pl}, t_{pl})f^{-\alpha(T_{pl}, t_{pl})} - \frac{1}{r_h}[Q(T_{pl}, t_{pl}, f) - Q(T_{pl}, 0, f)]$$

these conditions are easily transformed into

$$A^*(T_{pl}, t_{pl})f^{-\alpha(T_{pl}, t_{pl})} - (1/r_h)[Q^*(T_{pl}, t_{pl}, f) - Q^*(T_{pl}, 0, f)] > 0.$$

We now examine the question of derivability breaking [23]. The functions $\varepsilon^*(T_{pl}, t_{pl}, f)$ are not derivable against temperature (for $t_{pl} > 0$) if

$$\left(\frac{\partial \varepsilon^*}{\partial T}\right)_{T_{pl}=0} = P^*(T_{pl}, t_{pl}, f)_c \neq P^*(T_{pl}, t_{pl}, f)_h = \left(\frac{\partial \varepsilon^*}{\partial T}\right)_{T_{pl} \neq 0}.$$

Since

$$P^*(T_{pl}, 0, f)_c = P^*(T_{pl}, 0, f)_h$$

the derivability breaking conditions become

$$P^*(T_{pl}, t_{pl}, f)_c - P^*(T_{pl}, 0, f)_c \neq P^*(T_{pl}, t_{pl}, f)_h - P^*(T_{pl}, 0, f)_h.$$

Therefore, rejuvenation upon cooling and/or heating after aging implies derivability breaking. The conditions finally read

$$A^*(T_{pl}, t_{pl})f^{-\alpha(T_{pl}, t_{pl})} + B^*(T_{pl}, t_{pl})f^{-\beta(T_{pl}, t_{pl})} + \left(\frac{1}{r_h} - \frac{1}{r_c}\right)[L^*(T_{pl}, t_{pl})f^{-\lambda(T_{pl}, t_{pl})} - L^*(T_{pl}, 0)f^{-\lambda(T_{pl}, 0)}] \neq 0.$$

For $t_{pl} = 0$ the left-hand side is equal to 0. Otherwise, the first three terms are positive while the fourth term is negative and they may possibly cancel. However, since the exponents α , β and λ are not equal (indeed they depend in different ways on T_{pl} and t_{pl}) the left-hand side of this equation cannot be equal to 0 independent of frequency. Consequently, there is derivability breaking for $t_{pl} > 0$. These remarks about frequency are valid for rejuvenation upon cooling and/or heating after aging as well. In some sense, rejuvenation and derivability breaking are by-products of the frequency dependence.

7. Frequency analysis of memory

Memory is demonstrated by the difference between two curves both recorded during heating from T_{min} to T_{max} where T_{max} is an arbitrary temperature higher than T_{pl} . One follows a cooling interrupted by a plateau at T_{pl} while the other, taken as reference, follows a regular cooling (without plateau) from T_{max} to T_{min} . The difference, starting from a negative value due to aging at T_{pl} , first decreases, then passes through a minimum and finally increases.

The important dielectric constant values for the first curve are $\varepsilon(T_{min}, t_{pl} + \theta, f)$ and $\varepsilon(T_{pl}, t_{pl} + 2\theta, f)$ with $\theta = (T_{pl} - T_{min})/|r|$, which are respectively obtained when the temperature is at its minimum T_{min} and when it passes again through T_{pl} during heating. The two important values for the second curve are $\varepsilon(T_{min}, \theta, f)$ and $\varepsilon(T_{pl}, 2\theta, f)$.

Then we adopt as the measure of memory the complex quantity M defined as $M = [\varepsilon(T_{pl}, t_{pl} + 2\theta, f) - \varepsilon(T_{pl}, 2\theta, f)] - [\varepsilon(T_{min}, t_{pl} + \theta, f) - \varepsilon(T_{min}, \theta, f)]$.

We have studied memory in our two samples. Here too, we have found that in both samples this complex quantity obeys a frequency power law

$$M = D(T_{pl}, t_{pl}) f^{-\delta(T_{pl}, t_{pl})}.$$

In sample A, for $T_{pl} = 12.1$ K, $T_{min} = 4.8$ K and $t_{pl} = 10\,000$ s, the exponent is $\delta = 0.145 \pm 0.01$. It varies with T_{pl} and t_{pl} according to the two equations $\delta \cong 0.226 - 0.007T_{pl}$ and $\delta \cong 0.244 - 0.025 \log t_{pl}$. One may think that the exponent $\delta(T_{pl}, t_{pl})$ also depends on T_{min} since this temperature plays a part in the thermal history. In fact, we have found that it does not. We have observed that the efficiency of writing increases with t_{pl} (but seems to saturate for long times) and also increases with T_{pl} .

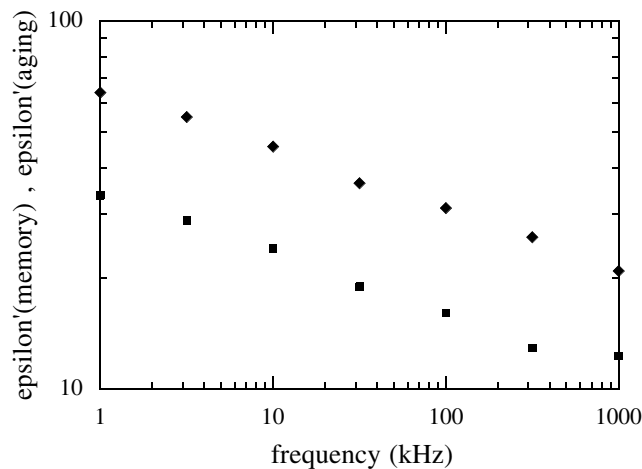


Figure 7. Log–log plot of the real part of memory (squares), as defined in the text, as a function of the frequency f measured in sample B after $t_{pl} = 10\,000$ s at $T_{pl} = 11.2$ K. The real part of the isothermal aging is also displayed (diamonds). The two sets of data points are parallel.

The results for sample B are shown in figure 7. They are analogous to those obtained on sample A [21]. The data points for memory (squares) and for aging (diamonds) fall on parallel straight lines. Another way to get evidence of this property is to display the two ratios of the real parts and of the imaginary parts. This is done in figure 8, which shows that the ratios are equal and do not depend on frequency. The important point is not the value of the ratios (which is contingent since it depends on the lowest temperature T_{min} and on the cooling rate) but that they are independent of frequency.

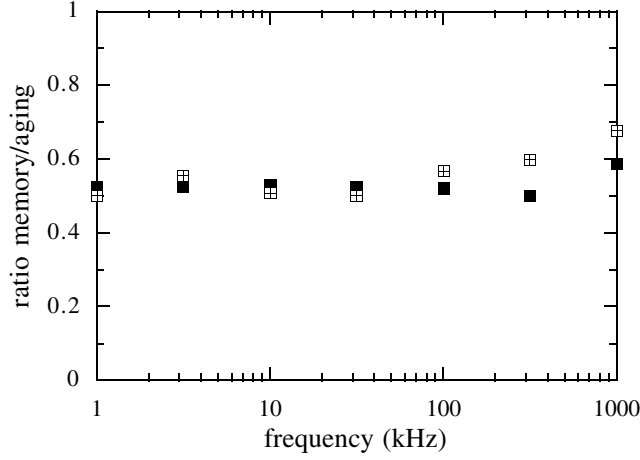


Figure 8. Semi-logarithmic plot of memory divided by aging (ratio of real parts: full squares; ratio of imaginary parts: open squares) as a function of the frequency f obtained in the conditions of figure 7. The two values are equal independent of frequency.

8. Relationships between some exponents

Up to this point, every exponent has been determined independently of the others. It may be worthwhile to look for some relationship which could exist between them. Indeed, we show below that the quasi-equality between ν and λ has a mathematical origin while the equality between ν and δ has a deep physical meaning, which can be interpreted within the domain model (see section 9).

8.1. Relation between exponents ν and λ

As noted in section 5.2, the difference $\Delta\varepsilon(T_{pl}, t_{pl}, f) = -Nf^{-\nu}$ is related to the evolution on the plateau, which reads $Q(T_{pl}, 0, f) = -L(T_{pl}, 0)f^{-\lambda(T_{pl}, 0)}$, by

$$\Delta\varepsilon(T_{pl}, t_{pl}, f) = \int_0^{t_{pl}} dt Q(T_{pl}, t, f).$$

Actually, ν depends on t_{pl} and the relation between ν and δ appears not to be simple, but it can be shown that $\nu = \lambda$ for $t_{pl} = 0$ and that they differ only by a logarithmic correction for $t_{pl} \neq 0$. This is confirmed by our measurements, which respectively provide $\nu = 0.23 \pm 0.005$ and $\lambda = 0.23 \pm 0.01$ for $t_{pl} \rightarrow 0$ and $T_{pl} = 12.1$ K (see section 4 and section 5.2).

8.2. Relation between exponents ν and δ

We have obtained that the exponent δ is $\delta = 0.145 \pm 0.01$ for $T_{pl} = 12.1$ K and $t_{pl} = 10\,000$ s (see section 7). This value is close to that obtained for ν in the same conditions (see section 4). Moreover the dependence of the two exponents ν and δ on the plateau duration t_{pl} and on the plateau temperature T_{pl} appears similar in the studied domain (see section 4 and section 7):

$$\begin{aligned} \nu &\approx 0.22 - 0.0063T_{pl} \text{ and } \delta \approx 0.226 - 0.007T_{pl} \text{ for } t_{pl} = 10\,000 \text{ s} \\ \nu &\approx 0.28 - 0.033 \log t_{pl} \text{ and } \delta \approx 0.244 - 0.025 \log t_{pl} \text{ for } T_{pl} = 12.1 \text{ K.} \end{aligned}$$

Therefore, the quasi-equality $\nu \cong \delta$ does not appear fortuitous. Indeed, it can be explained in the framework of a model recently proposed [21], which leads to the proportionality of memory and aging. This is developed in detail in section 9.

9. Model

It has been suggested [21, 24, 25] that the origin of aging in disordered ferroelectrics lies in the dynamics of domain walls pinned by impurities (here, the niobium atoms). With the concentration $y = 0.027$, the average distance between niobium atoms is 3.3 times the lattice parameter a . Owing to this high density of pinning impurities, ‘domain walls’ must not be understood in the usual sense: they are not planes along well defined crystallographic orientations which separate regions with different polarization directions; they must rather be thought of as tortuous elastic membranes which fluctuate and evolve from some anchorage points to others.

Motions of the walls arise by changing the direction of electric moments located at the border. Because of pinning by impurities, electric moments must overcome barriers of typical energy $\Psi(\ell/a)^z$ where ℓ is the linear length of a portion of wall, z an exponent depending on the dimensionality of the system and Ψ an energy scale. The time needed for a portion of wall with linear size ℓ to move is $\tau(\ell) = \tau_\infty \exp(\Psi(\ell/a)^z/(k_B T))$ [25]. This means that the portions of large lengths move much more slowly than those of small lengths. At a given temperature T and for a given lapse of time t a length ℓ_t can be defined by $\tau(\ell_t) \cong t$, in order that if $\ell < \ell_t$ reconformations of the walls at these small scales can take place during t while if $\ell > \ell_t$ all movements at these large lengths are frozen. In any case, the length ℓ is constrained by the two conditions $a \leq \ell \leq R$ where the domain size R can grow, at least in principle, without limit since the material is in a ferroelectric phase.

All these motions can be also described by the displacements of a representative point in the phase space of the sample [26, 27]. Then easy (short length) motions are represented by jumps over low barriers while difficult (large length) motions correspond to jumps over high barriers.

Two contributions to the time dependent dielectric susceptibility may be distinguished. The first one corresponds to small scale motions, which lead to better pinned configurations (wall reconformation) and a decrease of the susceptibility. The second contribution corresponds to motions at a length scale of the order of R , which induce the increase of the size (domain growth) and a correlative decrease of their number, and therefore a supplementary decrease of the susceptibility.

At the fixed temperature T_{pl} these two types of motion induce a therefore monotonic susceptibility decrease; this is isothermal aging. If the lapse t_{pl} at the temperature T_{pl} is long enough, two neighbouring conformations of energies E_1 and E_2 with $E_2 - E_1 = 2\Delta < k_B T_{pl}$ have practically reached their equilibrium occupation probabilities p_1 and p_2 such that $p_1 - p_2 = \tanh(\Delta/k_B T_{pl})$ and they no longer evolve; this also implies that the barrier between the conformations is not large in comparison with $k_B T_{pl}$. If now the temperature is decreased from T_{pl} to $T_{pl} - \Delta T$, the occupation probabilities must tend towards new values p'_1 and p'_2 where $p'_1 - p'_2 = \tanh(\Delta/k_B (T_{pl} - \Delta T))$ is larger than $p_1 - p_2$. Then relaxation is relaunched; this is rejuvenation. If the temperature is then increased back, conformations recover (at least in part) the state they had reached at T_{pl} ; this is memory.

Now we put on a more quantitative basis the evolution of the dielectric constant. After a plateau of duration t_{pl} at temperature T_{pl} it reads

$$\varepsilon(T_{pl}, t_{pl}, f) = \varepsilon_{st}(T_{pl}, \infty, f) + \frac{R(t_{pl})^2 \varphi_{rec}(T_{pl}, t_{pl}, f)}{R(t_{pl})^3}.$$

The first term $\varepsilon_{st}(T_{pl}, \infty, f)$ is the stationary (or asymptotic) dielectric constant, which may depend on the thermal history of the sample in case of ergodicity breaking. In the second term the numerator represents the surface domain contribution written as the average domain wall area multiplied by the factor $\varphi_{rec}(T_{pl}, t_{pl}, f)$, which takes into account the wall reformation; it is a decreasing function of t_{pl} which tends towards 0 if t_{pl} goes to infinity. The denominator originates from the domain density $R(t_{pl})^{-3}$. Finally, it reads

$$\varepsilon(T_{pl}, t_{pl}, f) = \varepsilon_{st}(T_{pl}, \infty, f) + \frac{\varphi_{rec}(T_{pl}, t_{pl}, f)}{R(t_{pl})}.$$

Accordingly, when the sample just arrives at T_{pl} , its dielectric constant is

$$\varepsilon(T_{pl}, 0, f) = \varepsilon_{st}(T_{pl}, \infty, f) + \frac{\varphi_{rec}(T_{pl}, 0, f)}{R(0)}.$$

Therefore, the aging part of the dielectric constant can be written

$$\Delta\varepsilon(T_{pl}, t_{pl}, f) = \varepsilon(T_{pl}, t_{pl}, f) - \varepsilon(T_{pl}, 0, f) = \frac{\varphi_{rec}(T_{pl}, t_{pl}, f)}{R(t_{pl})} - \frac{\varphi_{rec}(T_{pl}, 0, f)}{R(0)}.$$

The further procedure is composed of cooling below T_{pl} down to T_{min} and subsequent heating up to T_{pl} . Upon cooling from T_{pl} to T_{min} rejuvenation increases the dielectric constant and the previous isothermal aging apparently disappears. Upon heating from T_{min} to T_{pl} the memory of isothermal aging, which was hidden at T_{min} , is partly recovered. However, during this back and forth procedure non-isothermal aging occurs (it is cumulative because in a ferroelectric phase the domain size always increases, even if more slowly at low temperatures) and accordingly, the dielectric constant decreases. This is a spurious effect from our point of view, which consists in measuring the hidden memory only. In order to eliminate this artefact as well as possible we subtract from the data of our experiment the data of an experiment without memory, obtained with $t_{pl} = 0$, called the reference. Indeed the cancellation is not expected to be perfect since aging is not exactly the same for a young state ($t_{pl} = 0$) and an older one ($t_{pl} \neq 0$), but we assume that this approximation is good enough. This is why we have adopted the following definition of hidden memory:

$$M = [\varepsilon(T_{pl}, t_{pl} + 2\theta, f) - \varepsilon(T_{pl}, 0 + 2\theta, f)] - [\varepsilon(T_{min}, t_{pl} + \theta, f) - \varepsilon(T_{min}, 0 + \theta, f)]$$

with $\theta = (T_{pl} - T_{min})/r$.

Rejuvenation occurs because some short range motions which were in equilibrium at T_{pl} are no longer equilibrated upon cooling. Therefore $\varphi_{rec}(T_{pl}, t_{pl}, f)$ must be replaced by $\varphi_{rec}(T_{pl}, 0, f) > \varphi_{rec}(T_{pl}, t_{pl}, f)$. However, if all the domain walls have turned into young ones, nevertheless two types of domain have to be separated: the fastest of them have enough time to grow (therefore, they lose memory of their wall locations at T_{pl} before cooling) while the others are unable to significantly evolve (consequently they keep memory of their aging at T_{pl}). Let p (with $0 \leq p \leq 1$) be the probability that a wall does not move during the time 2θ elapsed at low temperatures $T < T_{pl}$. The parameter $p = p(\theta)$ measures the fraction of domains which retain memory; it is a decreasing function of θ .

The size of the domains which do not grow upon cooling after the plateau is naturally still written $R(t_{pl})$. Indeed, those which grow only undergo a weak change, sufficient to rule out the reversibility, but close enough to $R(t_{pl})$ so that they may be confused in most calculations; for these reasons we write $\tilde{R}(t_{pl})$ with $\tilde{R}(t_{pl}) \cong R(t_{pl})$. Similarly, if there is no plateau the two sizes are respectively written $R(0)$ and $\tilde{R}(0)$ with $\tilde{R}(0) \cong R(0)$. This notation is only a mnemonic of change, negligible or not according to the purpose.

The value of the dielectric constant after isothermal aging at T_{pl} , cooling down to T_{min} is

$$\varepsilon(T_{min}, t_{pl} + \theta, f) = \varepsilon_{st}(T_{min}, \infty, f) + p \frac{\varphi_{rec}(T_{min}, 0, f)}{R(t_{pl})} + (1 - p) \frac{\varphi_{rec}(T_{min}, 0, f)}{\tilde{R}(t_{pl})}$$

and after further heating from T_{min} up to T_{pl} , it reads

$$\varepsilon(T_{pl}, t_{pl} + 2\theta, f) = \varepsilon_{st}(T_{pl}, \infty, f) + p \frac{\varphi_{rec}(T_{pl}, t_{pl}, f)}{R(t_{pl})} + (1 - p) \frac{\varphi_{rec}(T_{pl}, 0, f)}{\tilde{R}(t_{pl})}$$

where it is assumed that $\varepsilon_{st}(T_{pl}, \infty, f)$ is unchanged, in agreement with temperature cycle experiments [10]. It is implied that rejuvenation upon cooling is reversible upon heating back if the domain size is not changed (the representative point stays in the same large valley in the phase space), while it is irreversible if the domain size is changed (the representative point has jumped into another large valley).

For the reference, where $t_{pl} = 0$, the dielectric constant respectively reads

$$\varepsilon(T_{min}, 0 + \theta, f) = \varepsilon_{st}(T_{min}, \infty, f) + p \frac{\varphi_{rec}(T_{min}, 0, f)}{R(0)} + (1 - p) \frac{\varphi_{rec}(T_{min}, 0, f)}{\tilde{R}(0)}$$

and

$$\varepsilon(T_{pl}, 0 + 2\theta, f) = \varepsilon_{st}(T_{pl}, \infty, f) + p \frac{\varphi_{rec}(T_{pl}, 0, f)}{R(0)} + (1 - p) \frac{\varphi_{rec}(T_{pl}, 0, f)}{\tilde{R}(0)}.$$

Therefore, the measure of memory defined in section 7 reads

$$\begin{aligned} M = & \left[p \frac{\varphi_{rec}(T_{pl}, t_{pl}, f)}{R(t_{pl})} + (1 - p) \frac{\varphi_{rec}(T_{pl}, 0, f)}{\tilde{R}(t_{pl})} \right] \\ & - \left[p \frac{\varphi_{rec}(T_{pl}, 0, f)}{R(0)} + (1 - p) \frac{\varphi_{rec}(T_{pl}, 0, f)}{\tilde{R}(0)} \right] \\ & - \left[p \frac{\varphi_{rec}(T_{min}, 0, f)}{R(t_{pl})} + (1 - p) \frac{\varphi_{rec}(T_{min}, 0, f)}{\tilde{R}(t_{pl})} \right] \\ & + \left[p \frac{\varphi_{rec}(T_{min}, 0, f)}{R(0)} + (1 - p) \frac{\varphi_{rec}(T_{min}, 0, f)}{\tilde{R}(0)} \right]. \end{aligned}$$

Subtracting the reference from the experiment was intended to (approximately) eliminate the cumulative non-isothermal aging. This implies that all the terms which contain the factor $(1 - p)$ should cancel each other. Indeed, since the growth process is much slower than the reformation process, the domain size hardly increases during the plateau and consequently $\tilde{R}(t_{pl}) \cong \tilde{R}(0)$. This results in the expected quasi-cancellation and this leaves only

$$M \cong p \left\{ \begin{array}{l} \frac{\varphi_{rec}(T_{pl}, t_{pl}, f)}{R(t_{pl})} - \frac{\varphi_{rec}(T_{pl}, 0, f)}{\tilde{R}(0)} \\ + \frac{\varphi_{rec}(T_{min}, 0, f)}{R(0)} - \frac{\varphi_{rec}(T_{min}, 0, f)}{\tilde{R}(t_{pl})} \end{array} \right\}.$$

Moreover, for the same reasons the last two terms in the preceding equation vanish:

$$M = p \left[\frac{\varphi_{rec}(T_{pl}, t_{pl}, f)}{R(t_{pl})} - \frac{\varphi_{rec}(T_{pl}, 0, f)}{\tilde{R}(0)} \right].$$

Finally, neglecting the growth which occurs during the short lapse θ , we get

$$M \cong p \left[\frac{\varphi_{rec}(T_{pl}, t_{pl}, f)}{R(t_{pl})} - \frac{\varphi_{rec}(T_{pl}, 0, f)}{R(0)} \right].$$

This important result also reads

$$M \cong p \Delta\varepsilon(T_{pl}, t_{pl}, f).$$

This means that memory M is proportional to aging $\Delta\varepsilon$. Therefore, since the probability p does not depend on frequency, M and $\Delta\varepsilon$ must have the same frequency dependence. This establishes that the two exponents δ and ν are equal, as experimentally observed.

It is worthwhile to compare our results on KTN to those obtained on the chromium thiospinel $\text{CdCr}_{1.9}\text{In}_{0.1}\text{S}_4$ [17]. This material presents a spin-glass phase (below 10 K) and a ferromagnetic phase (between 10 K and 68 K). Memory is fully recovered upon heating in the former while it is totally erased by domain growth in the latter. In the language used for our model it can be said that $p = 1$ in the spin-glass phase and $p = 0$ in the ferromagnetic phase for the conditions of the experiments. Then the ferroelectric phase of KTN (where $p \cong 0.5$ for our experimental conditions) appears as an intermediate case in which the weak domain growth only induces partial erasing or allows partial recovery.

10. Conclusion

We report on a detailed study of aging and of two associated effects, rejuvenation and memory, in the ferroelectric phase of KTN crystals, where some disorder was introduced by the randomly distributed invited niobium atoms. The frequency dependence of the dielectric constant has been measured over three frequency decades while the temperature and the duration of isothermal aging were varied. We propose a modified domain model able to account for the observed features. The model assumes that the dynamics of ε is due to the motions (growth and reformation) of the ferroelectric domain walls. The dynamics is slow because the wall motions are hindered by invited impurities (Nb^{5+} ions) acting as pinning sites.

A first important result is that the measured effects (aging, rejuvenation, memory etc) all obey power laws of frequency. A second important result is that the exponents δ and ν of the power laws for memory and aging are equal. This property is well explained in the framework of the model if it is assumed that the domains are split into two sub-sets according to their growth velocity: those with mobile enough walls so that they grow during the temperature sweep and the others which are practically frozen and hold memory. From this assumption, it follows that aging and memory after a temperature sweep are proportional and therefore have the same frequency behaviour.

Acknowledgments

We thank S Ziolkiewicz who grew the KTN crystals and J-P Bouchaud for fruitful discussions.

References

- [1] Struik L C E 1978 *Physical Aging in Amorphous Polymers and Other Materials* (Amsterdam: Elsevier)
- [2] Lundgren L, Svedlindh P, Norblad P and Beckman O 1983 *Phys. Rev. Lett.* **51** 911
- [3] Lefloch F, Hammann J, Ocio M and Vincent É 1992 *Europhys. Lett.* **18** 647
- [4] Vincent É, Hammann J, Ocio M, Bouchaud J-P and Cugliandolo L F 1997 *Sitges Conf. on Glassy Systems* ed M Rubi (Berlin: Springer)
- [5] Leheny R L and Nagel S R 1998 *Phys. Rev. B* **57** 5154
- [6] Kleemann W, Schönknecht V, Sommer D and Rytz D 1991 *Phys. Rev. Lett.* **66** 762
- [7] Alberici F, Doussineau P and Levelut A 1997 *J. Physique I* **7** 329
- [8] Alberici-Kious F, Bouchaud J-P, Cugliandolo L F, Doussineau P and Levelut A 1998 *Phys. Rev. Lett.* **81** 4987
- [9] Alberici-Kious F, Bouchaud J-P, Cugliandolo L F, Doussineau P and Levelut A 2000 *Phys. Rev. B* **62** 14 766
- [10] Doussineau P, de Lacerda-Arôso T and Levelut A 2000 *Eur. Phys. J. B* **16** 455
- [11] Colla E V, Chao L K, Weissman M B and Viehland D D 2000 *Phys. Rev. Lett.* **85** 3033
- [12] Knaebel A, Bellour M, Munch J-P, Viasnoff V, Lequeux F and Harden J L 2000 *Europhys. Lett.* **52** 73
- [13] Cloître M, Borrega R and Leibler L 2000 *Phys. Rev. Lett.* **85** 4819
- [14] Jonason K, Vincent É, Hammann J, Bouchaud J-P and Norblad P 1998 *Phys. Rev. Lett.* **81** 3243
- [15] Jonsson T, Jonason K, Jönsson P and Norblad P 1999 *Phys. Rev. B* **59** 8770
- [16] Doussineau P, de Lacerda-Arôso T and Levelut A 1999 *Europhys. Lett.* **46** 401

- [17] Vincent É, Dupuis V, Alba M, Hammann J and Bouchaud J-P 1995 *Europhys. Lett.* **50** 674
- [18] Cavailé J Y, Étienne S, Perez J, Monnerie L and Johari G P 1986 *Polymer* **27** 686
- [19] Bellon L, Ciliberto S and Laroche C 2000 *Europhys. Lett.* **51** 551
- [20] Doussineau P, de Lacerda-Arôso T and Levelut A 2000 *J. Phys.: Condens. Matter* **12** 1461
- [21] Bouchaud J-P, Doussineau P, de Lacerda-Arôso T and Levelut A 2001 *Eur. Phys. J. B* **21** 307
- [22] Fontana M D, Bouziane E and Kugel G E 1990 *J. Phys.: Condens. Matter* **2** 8681
- [23] Doussineau P and Levelut A 2000 *Europhys. Lett.* **52** 448
- [24] Bouchaud J-P and Dean D S 1995 *J. Physique I* **5** 265
- [25] Bouchaud J-P 2000 *Soft and Fragile Matter* ed E Cates and M R Evans (Bristol: Institute of Physics Publishing)
Bouchard J-P 1999 *Preprint* cond-mat/9910387
- [26] Dotsenko V S 1985 *J. Phys. C: Solid State Phys.* **18** 6023
- [27] Vincent É, Bouchaud J-P, Hammann J and Lefloch F 1995 *Phil. Mag. B* **71** 489